lubricants

MDPI

Article

Study on the Tribological Behaviors of a Wave Glider's Wing's Rotating Shaft Using Fractal and Chaotic Analysis

Shihui Lang [1,2,*], Hua Zhu [1] and Xuehai Lian [2]

[1] School of Mechanical and Electrical Engineering, China University of Mining and Technology, Xuzhou 221116, China; 13952207512@163.com
[2] China E-Tech (Ningbo) Maritime Electronics Research Institute Co., Ltd., Ningbo 315040, China; cetcme@139.com
* Correspondence: langshihuil@cumt.edu.cn; Tel.: +86-17851982708

Abstract: This paper conducts wear tests of rotating shafts and bearings, and collects the wear amount, surface morphology, and friction force signals to study its tribological behaviors using the fractal and chaotic analysis. The rotation shaft surface fractal dimension were calculated to characterize the self-similarity and smoothness, the signals' phase trajectories were constructed, and its correlation dimension and phase-point saturation were calculated to reveal the dynamic evolution of the system. The results show that the surface fractal dimension increases from low to high. The phase trajectory fluctuates and then maintains in a finite space, and the correlation dimension increases and stabilizes near the larger value while the phase-point saturation has the opposite evolution. The changes in surface fractal dimension, phase trajectories, correlation dimension, and phase-point saturation are similar to the wear rate, exhibiting a transition from instability to stability, which is more objective and sensitive than traditional representation methods. According to the fractal and chaotic characterization results of the worn surface and friction force signal, the material of CrNiMoN has better friction and wear properties than GCr15. The results reveal the tribological behaviors and wear mechanisms of the rotating shaft and provide guidance for material selection and designing, along with a basis for characterizing the wear status of the rotating shaft of wave glider wing.

Keywords: wave gliders; wing rotation shaft; tribological behaviors; fractal and chaos analysis

check for updates

Received: 20 February 2025
Revised: 21 March 2025
Accepted: 10 April 2025
Published: 16 April 2025

Citation: Lang, S.; Zhu, H.; Lian, X. Study on the Tribological Behaviors of a Wave Glider's Wing's Rotating Shaft Using Fractal and Chaotic Analysis. *Lubricants* **2025**, *13*, 185. https://doi.org/10.3390/lubricants13040185

Copyright: © 2025 by the authors. Licensee MDPI, Basel, Switzerland. This article is an open access article distributed under the terms and conditions of the Creative Commons Attribution (CC BY) license (https://creativecommons.org/licenses/by/4.0/).

1. Introduction

With the increasingly urgent demand for marine resource development and marine environment monitoring, all maritime powers in the world are constantly developing new sea survey monitoring tools to increase the monitoring ability of marine environment. As a new type of unmanned sea mobile platform, wave glider, as shown in Figure 1a, has the advantages of long sailing time and distance as well as high sea conditions [1–3]. The rotating shaft and the friction pair of bearing in the wave glider wing component (Figure 1b) are the key components of the wave glider, and their long-term operation and harsh working conditions directly affect the performance and life of the wave glider. Compared with the bearing wear, the rotating shaft wear is larger. Figure 1c shows the rotating shaft and bearing that were worn for one month. When the wear increases, the friction also increases, which decreases the efficiency of the wave gliders and the survival ability in the case of high sea conditions. Therefore, it is crucial to study the wear

characteristics of the wing rotation shaft of the wave glider to enhance its operation and maintenance and increase its sailing efficiency and overall service life.

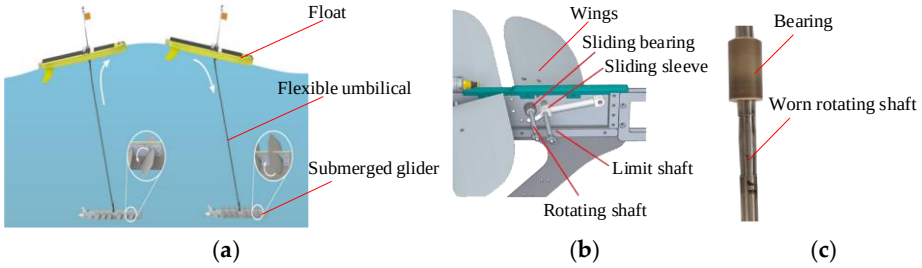


Figure 1. Wave glider, wing components and their rotating shaft, and bearing friction pair: (**a**) wave glider; (**b**) wing components and their rotating shaft; (**c**) bearing friction pair.

The traditional methods for studying the wear process of bearing friction pairs are mostly based on direct analysis of the amplitude changes in friction signals, such as the friction vibration and friction force. For instance, Kowalski et al. [4] studied the wear strength and reliability of shafts based on their wear amount and surface morphology information. Xu et al. [5] defined characteristic parameters that characterize wear using the friction vibration signals of rolling bearings. Savchenko et al. [6] studied the variation characteristics of acoustic emission signal energy with respect to the friction coefficient and degree of inverse transformation based on collected acoustic emission signals under forward and inverse transformations. Lychagin et al. [7] used fast Fourier transform to study the median frequency and energy of acoustic emission signals in slip systems at different friction stages. In addition, they established the relationship between the changes in the acoustic emission parameters and single crystal wear. Li et al. [8] analyzed the changes in friction current signals during the friction process of similar metal contact pairs, indicating that the trend of friction current changes during the friction process is consistent with the trend of friction coefficient changes. However, the studies on the characterization of wear processes based on wear amount and friction signal amplitude still have certain limitations. Furthermore, studying the state changes in friction and wear processes or predicting wear patterns by observing the amplitude changes in the output variables of the friction system may lose many useful nonlinear dynamic friction system information hidden in time series signals, making the observed and predicted results less objective. In addition, the measurement results of friction system output in traditional research are affected by instrument resolution and sampling length, which has an impact on the objectivity of the characterization results. Therefore, new methods are needed to characterize the wear process of the rotating shaft of wave glider wings.

Due to the continuous development and application of the nonlinear theory, the fractal and chaos theories were applied to the analysis of the dynamic characteristics of friction systems, as well as the identification and prediction of wear states. This provided new ideas and methods for studying complex problems in tribology. For instance, Zhou et al. [9] analyzed the relationship between running-in quality and the fractal dimensions of friction signal and wear surface. The result shows that the larger the fractal dimension, the higher the running-in quality. Zuo et al. [10] calculated surface roughness and multifractal spectrum parameters to characterize the wear morphology characteristic and its different wear mechanisms. Lu et al. [11] calculated the Lyapunov exponent, Kolmogorov entropy, and average distance between phase points based on the reconstructed phase space. The results indicate that all chaotic features can distinguish different alignment states of the shaft system. Sun et al. [12] applied chaos theory to study the attractors of friction vibration and analyzed the evolution mechanism of the chaotic attractors of friction vibration during the running-in process. Their results showed that friction vibration is chaotic, and the

chaotic attractors in phase space are always trajectories with specific levels and structures. Wang et al. [13] used fractal dimension, multifractal parameters, and correlation dimension to extract nonlinear features of worn surfaces and friction coefficients and evaluated their running-in quality. Xing et al. [14] studied the chaotic characteristics of the friction forced vibration of bearings based on vortex attractors, focusing on characterizing the evolution process and revealing their evolution mechanism. Peng et al. [15] used chaos theory to analyze the dynamic characteristics of friction coefficients for the detection and identification of bearing running in state. Mevel et al. [16] used chaos theory to identify and predict the operating state of bearing systems. Ye et al. [17] effectively integrated chaos theory, the gray bootstrap method, and the maximum entropy method to establish a mathematical model for evaluating the dynamic uncertainty of rolling bearing vibration performance and then predicted the vibration performance of rolling bearings. Xia et al. [18] studied the variation characteristics of friction torque and the diversity and complexity of attractors in phase space based on chaos theory and vacuum variation experiments. Zhou et al. [19,20] quantitatively characterized the running-in state of the friction system and the variation patterns of the wear process based on parameters such as the correlation dimension and predictability of friction coefficient and friction force signals. Ding et al. [21] characterized the chaotic characteristics of the friction coefficient signal generated by the friction system and identified and predicted the wear state of the friction system through the evolution law of the chaotic feature quantity. However, the fractal and chaos theories have not been used in the study of wear caused by seawater corrosion, and due to the influence of environmental factors on bearing pairs, the amplitude changes in friction signals make it difficult to objectively characterize the wear state. In order to improve its online characterization accuracy based on the wear surface and friction force signal, the wear process is investigated using fractal and chaos theory.

This paper introduced the fractal and chaotic theory to investigate the friction pair wear process of the wave glider rotation shaft and bearing friction pair. Wear tests were conducted on rotation shafts and bearings made of different materials, and the friction signals were collected. The fractal and chaotic characterization methods were introduced for characterizing the wear surface morphology and friction signals of the rotating shaft. The state changes and dynamic evolution laws of the grip wear process were revealed, demonstrating tribological behavior. This provides a theoretical basis for the wear resistance, long-term effectiveness, and reliability design of the rotating shaft of wave glider wings.

2. Wear Test and Result Analysis

2.1. Test Equipment and Specimens

In order to study the wear performance of existing materials, wear tests were conducted on two different shaft materials and Peek bearing materials on an FTM tribometer. Surface morphology measurements were performed using a JB-5C surface contour measuring instrument (Shanghai Taiming Optical Instrument Co., Ltd., Shanghai, China), and the wear amount was weighed using a high-precision electronic scale. The wear tests specimen and its fixture are shown in Figure 2.

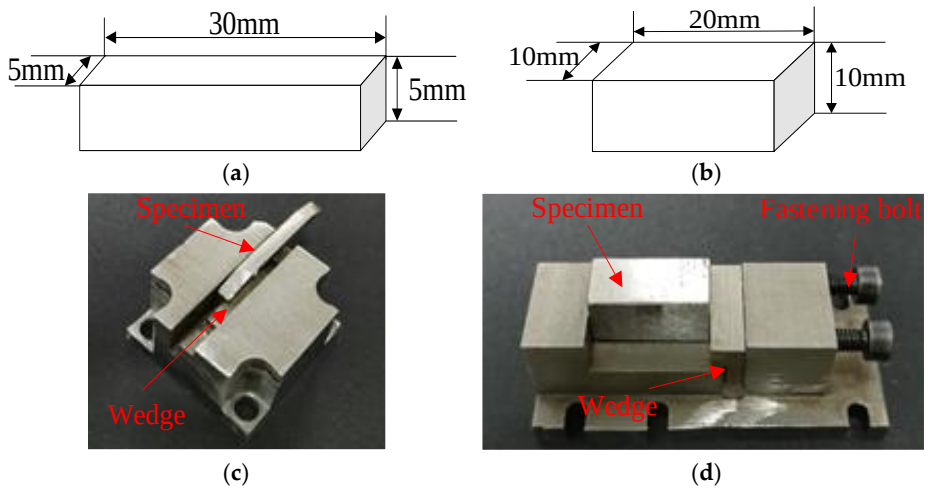


Figure 2. The specimen and its fixture: (**a**) upper specimen; (**b**) lower specimen; (**c**) upper specimen fixture; (**d**) lower specimen fixture.

2.2. Test Method

The two sets of friction pair materials for the wear test are shown in Table 1.

Table 1. Two sets of friction pair materials.

Number	1	2
Upper specimen material	GCr15	CrNiMoN
Lower specimen material	Peek	Peek

Due to the action of waves, the wave glider wing moves every 6 s or so, and the reciprocating motion of the shaft in the bearing is approximately between 20° and −90°, and the reciprocating stroke of sliding is 4.5 mm. The wing needs to move more than 1.5 million times in a 6-month maintenance cycle. Therefore, considering the working characteristics of the rotating shaft of the wave glider wing, the load is set to 20 N and the reciprocating stroke is 4.5 mm. In order to increase the efficiency of the test, a reinforced test design with a reciprocating frequency of 20 Hz was adopted, and the length of each test was set to 21 h based on a maintenance cycle. In order to collect information on the surface morphology and wear amount of the friction pair, an offline shutdown method was used to collect the contour curve of the worn surface morphology every 2 h, and a torque sensor was used to collect the friction force signal.

2.3. Test Results and Analysis

2.3.1. Wear Amount and Wear Rate

Figure 3 shows the average wear amount and wear rate of the friction pair during the wear process of the rotation shaft and bearing specimens.

With the progress of the wear process, the wear amount of the shaft and bearing samples gradually increases, and the wear rate first gradually decreases and then stabilizes around a small value. In the initial wear stage, the wear amount of the wing rotating shaft and bearing specimens is small and the wear rate in the initial wear stage is relatively high. As the wear process progresses, the amount of wear gradually increases, and its surface morphology gradually becomes smooth. The friction pair reaches a stable state. Although the amount of wear continues to increase, the wear rate will decrease and stabilize around a smaller value. The wear rate around 0.5×10^{-3} g/h in the stable stage is less than the running-in stage for Test 1, and the wear rate of CrNiMoN is less than GCr15, which indicate that CrNiMoN has a better wear resistance. In addition, the experiment results can

reduce the high cost and cycle of long-term offshore testing and improve the research and development efficiency of new materials and structures.

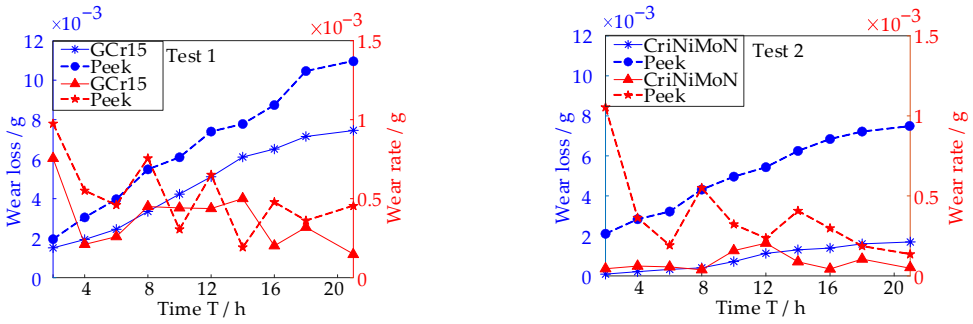


Figure 3. Changes in wear amount and wear rate of shaft and bearing specimens: (**a**) Test 1; (**b**) Test 2.

2.3.2. Wear Surface Morphology

Figure 4 shows the worn surface morphology during the wear process. Note that due to space limitations, only the worn surface morphology of the wear process of the Test 1 rotation shaft specimen is presented.

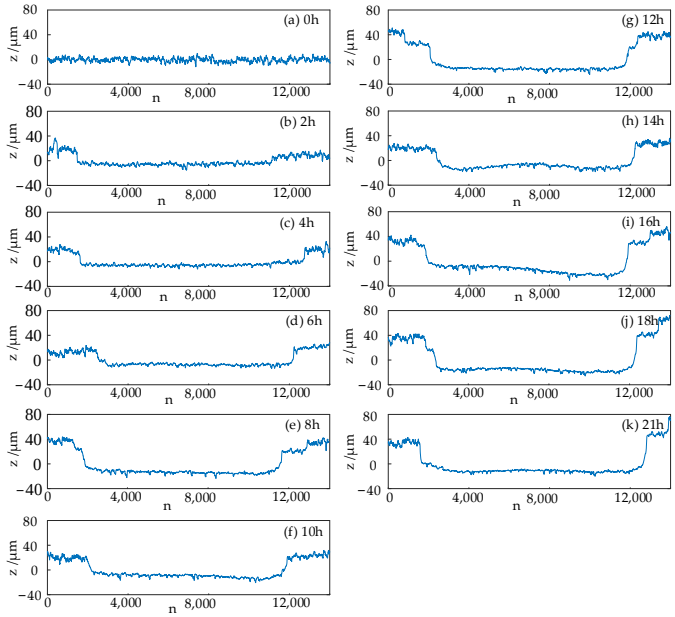


Figure 4. Worn surface of GCr15 rotation shaft specimen during wear process in Test 1.

It can be seen that the wear depth of the shaft specimen gradually increases, and the worn surface gradually becomes smooth. At the initial stage, slight scratches and wear depth exist on the surface of the shaft specimen. As the wear process progresses, the depth and width of the shaft wear gradually deepen and expand, and its surface morphology changes from rough to smooth, leading to the formation of a stable surface morphology structure. The results of the simulated acceleration test wear depth changes of the CrNiMoN material compared with the actual working conditions of GCr15 are smaller, which indicates that CrNiMoN has good wear resistance.

2.3.3. Friction Force Signals

Collect the friction force signals of the friction pair during the wear process at different time periods in Test 1, as shown in Figure 5.

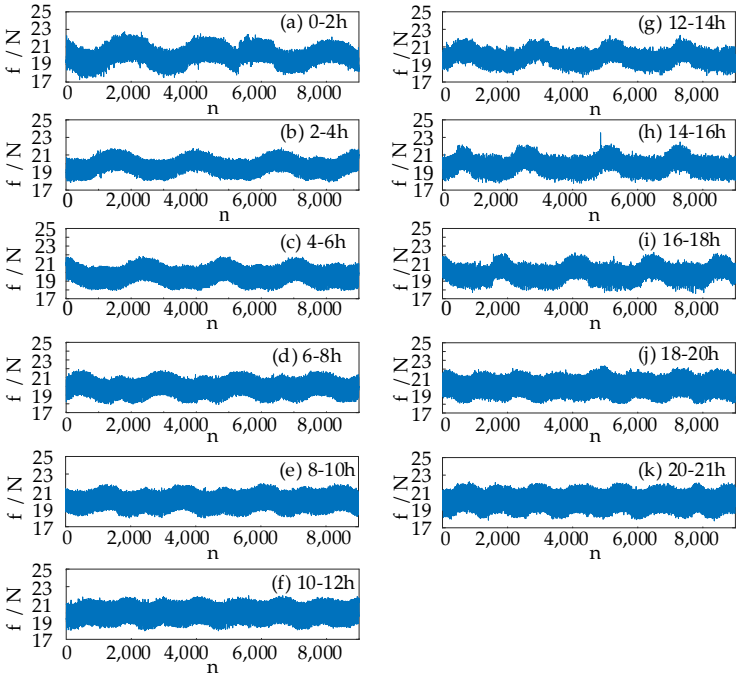


Figure 5. Friction force signals during wear process of Test 1.

It can be seen that the amplitude of the friction force signal oscillates and then gradually stabilizes around a certain value during the wear process. It can be deduced from the evolution of the wear amount, surface morphology, and friction force signal that in the initial wear stage, the meshing and shearing of rough peaks on the harder and softer surfaces of the friction pair generate new abrasive particles and material migration, which results in a higher wear rate. In addition, due to the rough contact surface and high friction force, the friction pair is in an initial unstable state. As the wear process progresses, the roughness peak of the worn surface gradually decreases, the generated abrasive particles and material migration become small, the wear rate becomes low, the contact surface gradually becomes smooth, the range of friction force fluctuations gradually decreases, and the friction system gradually converges to a stable state. The obtained results show that the wear amount, wear rate, surface roughness, and friction force signal have consistent variation patterns.

3. Results

The device resolution and sampling length affect the measured wear amount, wear rate, wear surface morphology information, and changes in friction force amplitude, which has an impact on the objectivity of the characterization results. For example, although the amplitude of the friction signal varies to some extent, its variation is not significant enough. Therefore, the analysis of the amplitude change cannot accurately reveal the complex dynamic behavior hidden in the friction system. To solve the aforementioned problems, the dynamic characteristics of the wear process of the wave glider wing bearing pair are characterized by introducing fractal and chaos characterization methods.

3.1. Fractal Characterization Method for Worn Surfaces

The fractal dimension (a fraction) is the characteristic quantity of fractals. The surface morphology is the fractal characteristic object in friction systems. Its fractal dimension is usually calculated using the structure function method [22]. The structural function

method equates the surface contour curve $Z(x)$ to a time series, and its structural function satisfies the following:

$$S(\tau) = [Z(x+\tau) - Z(x)]^2 = C\tau^{4-2D_s} \quad (1)$$

where $[Z(x+\tau) - Z(x)]^2$ is the arithmetic mean $S(\tau)$ of the difference, τ is the scale, which is any value of the data interval, D_s is the fractal dimension of the contour structure function, and C is the scale coefficient.

The $S(\tau)$ of the contour curve for several scales τ is calculated to determine the relationship between the fractal parameter D_s and τ in the structural function method, as shown in Figure 6. Therefore, considering the logarithm on the two sides of Equation (1), slope α of line $\ln S(\tau) - \ln \tau$ is obtained in a logarithmic scale, and its relationship with D_s is given by the following:

$$D_s = 2 - \alpha/2 \quad (2)$$

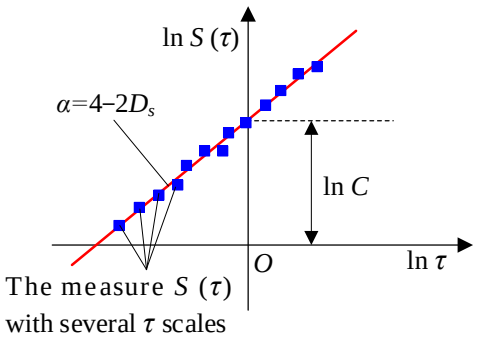


Figure 6. Double logarithmic relationship between D_s and τ in structural function method.

The fractal dimension is a characteristic quantity describing the irregularity and scale-free nature of complex systems. It can quantitatively analyze and characterize the microstructure of bearing pairs' wear surfaces.

3.2. Chaos Characterization Method for Friction Signals

A friction system composed of rotating shaft and bearings of the wave glider wing is a complex nonlinear system with the general characteristics of chaotic systems. It can be characterized by phase trajectory, correlation dimension, and phase-point saturation methods.

3.2.1. Phase Trajectory Method

The phase space reconstruction technique is used to reconstruct the collected friction signals [23]. The evolution process of the attractor phase trajectory of the friction system is studied in the reconstructed high-dimensional space. In phase space reconstruction, the embedding dimension parameters are usually determined using the False Nearest Neighbor method [24,25], while the time delay uses the autocorrelation function method [26]. In addition, principal component analysis is applied to project the attractor phase trajectory onto the U, V, and W vector directions [27].

3.2.2. Correlation Dimension Method

Correlation dimension (D_2) is a type of fractal dimension. It is sensitive to the evolution of the system over time, and it can objectively reflect the dynamic characteristics of complex systems. The G-P algorithm is a classic algorithm for calculating correlation dimension

due to its high efficiency, robustness, and universality. And D_2 is calculated using the G-P method [28]. In m-dimensional space, the correlation integral $C(r)$ is computed as follows:

$$C(r) = \frac{1}{N(N-1)} \sum_{i=1}^{N} \sum_{j=1, i \neq j}^{N} \left[H\left(r - \left\| X_i - X_j \right\|\right)\right] \tag{3}$$

where $H(\cdot)$ is the unit step function, r is a small scalar greater than zero, X_i is the reconstructed phase space vector, and N is the number of reconstructed phase space vectors.

Moreover, D_2 is defined as follows:

$$D_2 = \lim_{r \to 0} \frac{\ln C(r)}{\ln r} \tag{4}$$

A curve under the double logarithmic coordinate $\ln C(r) - \ln r$ can be obtained, and the slope of the fitting line is the correlation dimension D_2. To use the test as an example, the result is shown in Figure 7.

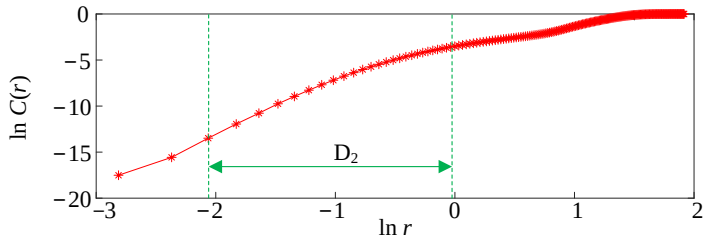


Figure 7. Double logarithmic curve of D_2 in Test 1.

3.2.3. Phase-Point Saturation Method

The phase-point saturation parameter is equivalent to the capacity dimension to describe the stable state for friction pairs. That is, the infinitesimal point is equivalent to the phase-point in phase space to measure the saturation degree of the measured object in the system, so it is called phase-point saturation S_p. This is computed as follows [29]:

$$S_p = \frac{V_{max} = \pi \max(|\boldsymbol{X}_i - \boldsymbol{O}_o|)^3 / 6}{N_P} \tag{5}$$

where $\boldsymbol{O_o}$ is the center point coordinates, $N_p = N$.

3.3. Fractal and Chaos Characterization Method for Friction Signals

3.3.1. Fractal Characterization Results and Analysis of Worn Surfaces

The fractal dimension D_s of the worn surface morphology of the shaft and bearing during the wear process was calculated using the method described in Section 3.1, and the results are shown in Figure 8.

It can be seen that, as the wear process progresses, D_s of the GCr15 and CrNiMoN shaft specimens first increases and then stabilized near a large value. However, D_s of the Peek surface in Test 1 oscillates, while that of the Peek surface in Test 2 first increases and then decreases. D_s describes the complex geometric structure of worn surfaces. The higher its value, the higher the surface self-similarity and smoothness, which indicates that worn surfaces have an evolution law from roughness to smoothness. This also reflects the complexity and evolution process of worn surfaces. The larger D_s represents the smoothness and high self-similarity of the surface, indicating that the surface state is stable. Thus, CrNiMoN is more wear-resistant compared with GCr15 in the process.

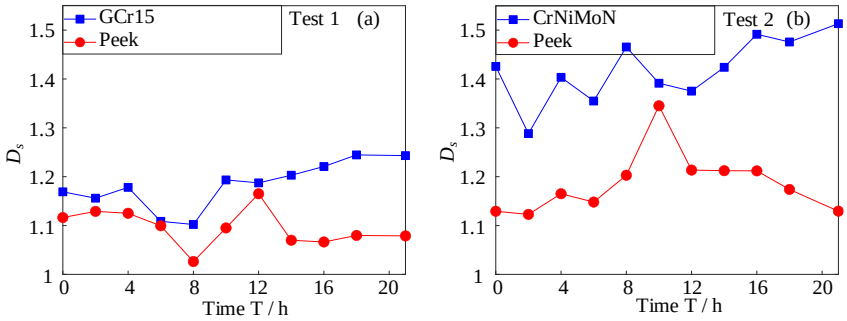


Figure 8. The worn surface morphology fractal dimension of the shafts and bearings: (**a**) Test 1; (**b**) Test 2.

3.3.2. Chaos Characterization Results and Analysis of Wear Process

Using the method introduced in Section 3.2, phase trajectories were constructed and correlation dimension D_2 and phase-point saturation S_p were calculated for two sets of friction signals. The concept of the time window was used to construct phase trajectories, with the data volume corresponding to 2 h as one time window. The results are shown in Figure 9. Due to space limitations, only the Test 1 phase trajectories are displayed.

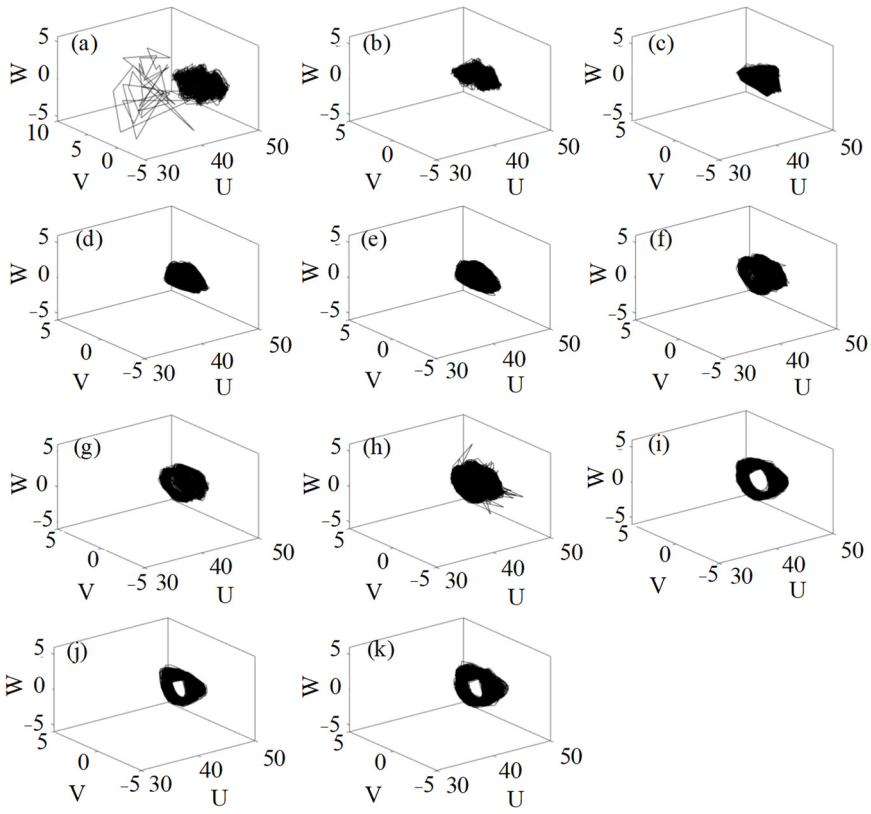


Figure 9. Evolution law of phase trajectories constructed from friction force signals in Test 1: (**a**) 0–2 h; (**b**) 2–4 h; (**c**) 4–6 h; (**d**) 6–8 h; (**e**) 8–10 h; (**f**) 10–12 h; (**g**) 12–14 h; (**h**) 14–16 h; (**i**) 16–18 h; (**j**) 18–20 h; (**k**) 20–21 h.

It can be seen from Figure 9 that the phase trajectory volumes in Test 1 exhibit an increasing evolution law. It then gradually increases and stabilizes in a finite spatial range. The phase trajectory line evolves from initial disorder towards a stable structure, and performs a circular motion near a fixed point, presenting a single spiral curve structure. These spiral lines are constrained to interlace within a limited spatial area, where their trajectories gradually converge and reach a steady-state equilibrium state, revealing the complex structural features and their evolution processes and behaviors that are hidden in

high-dimensional space. The phase trajectories of the friction force signal in Test 2 follows the same evolution law as that of Test 1.

The D_2 and S_p results are shown in Figure 10.

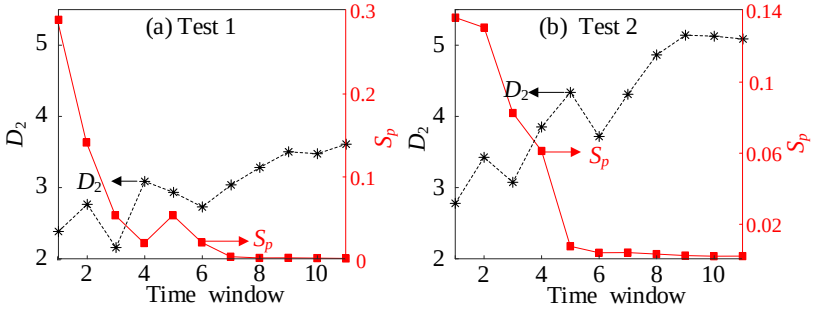


Figure 10. Evolution law of D_2 and S_p of friction force signals.

It can be observed from Figure 10 that D_2 increases and then gradually stabilizes around large values, and S_p has the opposite evolution. In the initial wear stage, D_2 is low, and the low self-similarity between adjacent states indicates that the system is in an unstable divergent state. As the wear process progresses, D_2 gradually increases then stabilizes near a large value. The high self-similarity of the represented adjacent states indicates that the system is in a stable convergence state. This reveals the process of the chaotic behavior evolution of the friction system (i.e., from being far away from the equilibrium state to reaching the equilibrium state).

The characterization results indicate that the evolution of friction signals and their D_2 and S_p during the wear process is consistent with the evolution of phase trajectories and the fractal dimension of the wear surface. Therefore, they can objectively characterize and identify changes in the wear state. The larger D_2 and smaller S_p indicate that the system enters a stable state, while conversely, the system is unstable. Therefore, online monitoring of changes in D_2 and S_p can effectively monitor changes in the system's status. Thus, it can be proved that CrNiMoN is more stable compared with GCr15 in the process. The values of D_s, D_2, and S_p can be used to evaluate the quality of the wear process and also provide evaluation indicators for material selection.

4. Discussion

The wear characteristics of the wing bearings of wave gliders have similar mechanisms as [30], which are affected by abrasive wear and adhesive wear; the corrosion wear is an exception, which leads to a more complex wear phenomenon with multi-factors. Firstly, during navigation, the coupling effect of axial force, radial force, friction force, and vibration impact force on the wing bearings of wave gliders can lead to increased wear of the bearings. The dynamic changes in the wear process are shown in Figure 11.

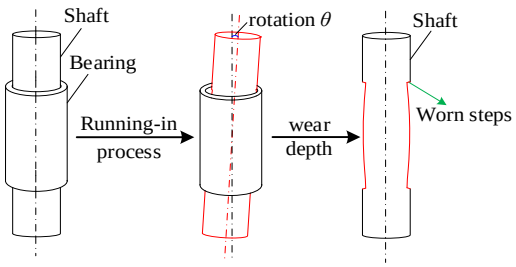


Figure 11. Dynamic changes in the wear process between the wing rotating shaft and the bearing.

During the wear process, the wear degree of the rotating shaft and bearings constantly changes under the coupling impact of axial force, radial force, friction force, vibration impact force, and corrosion, which contributes to the unbalanced 2D worn surface morphology shown in Figure 12.

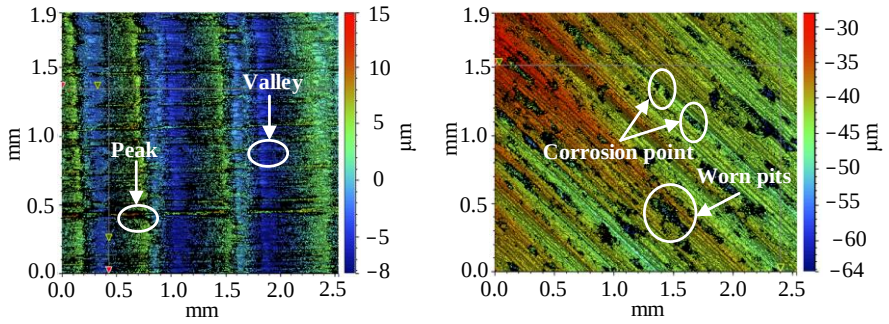


Figure 12. The three-dimensional worn morphology of the CGr15 rotation shaft specimen: (**a**) the initial surface morphology; (**b**) the worn morphology after 18 h.

It can be seen from Figures 11 and 12 that, in the initial running-in stage, the wear amount and inter axis clearance between the rotating shaft and the bearing are small, and small wear marks exist on the rotating shaft surface. The created friction force is also small and significantly fluctuates, and the friction pair surface is rough. The actual contact area and the number of contact points are small, while the area of most of the contact points is large. The adhesion of contact points is severe. Therefore, the wear rate is large, the surface fractal dimension, correlation dimension and phase-point saturation significantly change, and the range of phase trajectory movement is large. The wear process is unstable and the system diverges at this time. In addition, as the wear process progresses, although the wear amount of the bearing gradually increases, and even small wear steps may appear, the traces on the wear surface of the rotating shaft gradually stabilize. This results in forming a stable worn surface with the coupling effect of corrosion and abrasive wear; the wear mechanism of the rotation shaft and bearing pairs are shown in Figure 13.

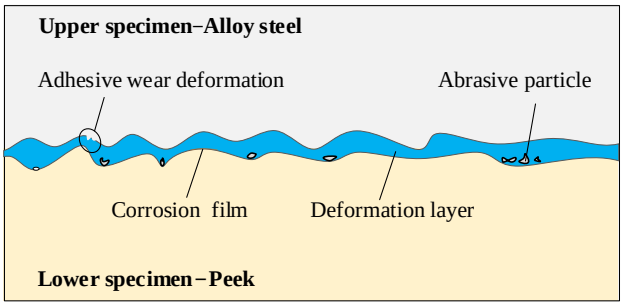


Figure 13. The wear mechanism of the rotation shaft and bearing pairs.

It can be seen from Figure 13 that the bearing pair of the alloy steel and Peek formed a deformation layer with generating abrasive particle, adhesive wear deformation, and corrosion film. During the wear process, the micro protrusions on the surface are gradually worn away, the surface roughness decreases, the actual contact area increases, the number of contact points increases, and the wear rate decreases. Due to the increase in the gap between the rotating shaft and the bearing, the friction force increases to a certain extent. However, the amplitude does not significantly fluctuate, and it stabilizes near a certain value. At this time, the surface fractal dimension and correlation dimension values are large, the range of phase trajectory motion is small, and a stable structure is formed. When

the system gradually reaches a stable state, it converges. In addition, CrNiMoN has the same law in the running-in process. The difference between CrNiMoN and GCr15 is that the corrosion and abrasive wear coupling effect of the former is small, and its friction performance is higher.

5. Conclusions

To study the wear characteristics and dynamic evolution laws of the rotating shaft wear process of wave glider wing blades, this paper conducted wear tests on rotating shaft and bearing samples made of CrNiMoN and GCr15 alloy steel materials. The wear amount, surface morphology, and friction signal during the wear process were collected, and the fractal dimension of the worn surface was calculated. The phase trajectory of the friction signal was constructed, the correlation dimension and phase-point saturation were calculated. The main conclusions are as follows:

(1) During the wear process of the rotating shaft and bearing specimen of the wave glider wing, the wear amount, surface morphology, and evolution law of friction force signals are consistent. The wear amount increases, the wear rate decreases, the worn surface morphology changes from rough to smooth, and the friction force signal first decreases and then increases. These friction and wear information indicate that the wear process of the bearing pair consists of changing from an unstable state in the initial wear stage to a stable convergence state. The result indicates that CrNiMoN has better wear resistance than CGr15.

(2) By introducing the fractal and chaos theory, the fractal dimension of surface morphology, correlation dimension, and phase-point saturation of friction force signals are calculated, and the phase trajectory is constructed. The obtained results show that the range of phase trajectory motion follows an evolutionary law of significantly decreasing and then maintaining a finite phase space. The surface fractal dimension and correlation dimension first increase then gradually stabilize around large values, whereas phase-point saturation is the opposite, revealing the dynamic evolution process of the wear changing from an unstable divergent state to a stable convergent state in time and space. These results indicate that CrNiMoN has better wear resistance and quality than GCr15.

(3) Therefore, the use of fractal and chaotic characterization methods can objectively describe friction systems of high complexity, irregularity, and nonlinear characteristics, without being affected by the device resolution and sampling length. This provides new ideas and methods for the identification of the wear state and the characterization of the wear characteristics of wave glider wing rotation shafts. CrNiMoN is more suited to the be used in the wing bearing of a wave glider compared with GCr15. Thus, the method can be used to make a selection for different material designs based on the worn surface and friction force signals in other industrial friction pairs with a multi-factor coupling effect.

(4) The quality evaluation and state characterization of the wear process can be applied to other complex friction systems. The stronger and more complex the nonlinearity of the system, the more advantageous the characterization results will be. By identifying and monitoring the state of the wear process, timely measures can be taken to extend the service life of the shaft, increase the reliability and operational efficiency of the wave glider, and provide a certain theoretical basis and practical guidance for future studies in this field.

Author Contributions: Conceptualization, S.L., H.Z. and X.L.; methodology, S.L.; software, S.L.; validation, S.L. and X.L.; formal analysis, X.L.; investigation, S.L.; resources, X.L.; data curation,

S.L.; writing—original draft preparation, S.L.; writing—review and editing, S.L.; visualization, S.L.; supervision, H.Z.; project administration, X.L.; funding acquisition, S.L. All authors have read and agreed to the published version of the manuscript.

Funding: This research was funded by the National Natural Science Foundation of China, grant number 51775546; the Fundamental Research Funds for the Central Universities (Grant no. 2024QN11018); the Jiangsu Funding Program for Excellent Postdoctoral Talent (2024ZB585); and the Priority Academic Program Development of Jiangsu Higher Education Institutions (PAPD).

Data Availability Statement: The original contributions presented in the study are included in the article, further inquiries can be directed to the corresponding author.

Acknowledgments: The authors gratefully acknowledge all the professors for their guidance and help during testing and writing.

Conflicts of Interest: Authors Shihui Lang and Xuehai Lian were employed by the company China E-Tech (Ningbo) Maritime Electronics Research Institute Co., Ltd. The remaining author declares that the research was conducted in the absence of any commercial or financial relationships that could be construed as a potential conflict of interest.

References

1. Zhang, J.; Chang, Z.; Lu, G.; Zheng, Z.; Zhang, Z. Analysis of the dynamic system of wave glider with a towed body. *J. Ocean Univ. China* **2020**, *19*, 519–524. [CrossRef]
2. Wang, P.; Wang, D.; Zhang, X.; Guo, X.; Li, X.; Tian, X. Path following control of the wave glider in waves and currents. *Ocean Eng.* **2019**, *193*, 106578. [CrossRef]
3. Wang, P.; Wang, D.; Zhang, X.; Li, X.; Peng, T.; Lu, H.; Tian, X. Numerical and experimental study on the maneuverability of an active propeller control based on wave glider. *Appl. Ocean Res.* **2020**, *104*, 102369. [CrossRef]
4. Kowalski, S.; Pexa, M.; Aleš, Z.; Čedík, J. Failure Analysis and the Evaluation of Forced-in Joint Reliability for Selected Operation Conditions. *Coatings* **2021**, *11*, 1305. [CrossRef]
5. Xu, C.; Li, B.; Wu, T. Wear characterization under sliding–rolling contact using friction-induced vibration features. *Proc. Inst. Mech. Eng. Part J J. Eng. Tribol.* **2022**, *236*, 634–647. [CrossRef]
6. Savchenko, N.L.; Filippov, A.V.; Tarasov, S.Y.; Dmitriev, A.I.; Shilko, E.V.; Grigoriev, A.S. Acoustic emission characterization of sliding wear under condition of direct and inverse transformations in low temperature degradation aged Y-TZP and Y-TZP-Al_2O_3. *Friction* **2018**, *6*, 323–340. [CrossRef]
7. Lychagin, D.V.; Filippov, A.V.; Kolubaev, E.A.; Novitskaia, O.S.; Chumlyakov, Y.I.; Kolubaev, A.V. Dry sliding of had field steel single crystal oriented to deformation by slip and twinning: Deformation, wear, and acoustic emission characterization. *Tribol. Int.* **2018**, *119*, 1–18. [CrossRef]
8. Li, G.; Yang, S.; Xing, P.; Liu, T.; Gao, H.; Song, Y.; Zhang, H. Experimental Investigation of Triboelectrification Behaviour in the Friction Process. *Lubricants* **2022**, *10*, 180. [CrossRef]
9. Zhou, Y.; Wang, Z.; Zuo, X. Multi-Objective Optimization of Three-Stage Running-In Process for Main Bearing of Marine Diesel Engine. *J. Tribol.* **2023**, *145*, 081701. [CrossRef]
10. Zuo, X.; Xie, W.; Zhou, Y. Influence of Electric Current on the Wear Topography of Electrical Contact Surfaces. *J. Tribol.* **2022**, *144*, 071702. [CrossRef]
11. Lu, L.; Li, G.; Xing, P.; He, W.; Feng, Z.; Zhang, H. Investigation on alignment state evolution of ship propulsion shafting based on chaotic characteristics of vibration signals. *Ocean Eng.* **2025**, *322*, 120521. [CrossRef]
12. Sun, D.; Li, G.; Wei, H.; Liao, H. Experimental study on the chaotic attractor evolvement of the friction vibration in a running-in process. *Tribol. Int.* **2015**, *88*, 290–297. [CrossRef]
13. Wang, Z.; Zhou, Y.; Zuo, X. Tribological effect of ZBUP additive on the running-in quality of sliding bearing by fractal analysis. *Ind. Lubr. Tribol.* **2022**, *74*, 1165–1173. [CrossRef]
14. Xing, P.; Li, G.; Gao, H.; Gao, H.; Lu, L.; Yang, S.; Zhang, H. Experimental investigation on the scroll attractor evolvement of friction-induced vibration under the different friction conditions. *Mech. Syst. Signal Process.* **2022**, *168*, 108725. [CrossRef]
15. Peng, M.; Zhou, Y.; Zuo, X. Application of recurrence dynamic analysis to running-in state recognition. *Ind. Lubr. Tribol.* **2021**, *73*, 756–764. [CrossRef]
16. Mevel, B.; Guyader, J. Experiments on routes to chaos in ball bearings. *J. Sound Vib.* **2008**, *318*, 549–564. [CrossRef]
17. Ye, L.; Xia, X.; Chang, Z. Evaluation of dynamic uncertainty of rolling bearing vibration performance. *Math. Probl. Eng.* **2019**, *2019*, 2896046. [CrossRef]

18. Xia, X.; Chen, L.; Fu, L.; Li, J. Information mining for friction torque of rolling bearing for space applications using chaotic theory. *Res. J. Appl. Sci. Eng. Technol.* **2013**, *5*, 5223–5229. [CrossRef]
19. Zhou, Y.; Tang, X.; Zuo, X. Prediction model of fractal dimensions in steady state through a multi-stage running in of Sn11Sb6Cu and AISI 1045 steel. *Wear* **2021**, *477*, 203770. [CrossRef]
20. Zhou, Y.; Zhu, H.; Zuo, X. The Behavior of intrinsic randomness and dynamic abrupt changes of friction force signal during the friction process. *J. Tribol.* **2016**, *138*, 031605. [CrossRef]
21. Ding, C.; Feng, S.; Qiao, Z.; Zhu, H.; Zhou, Z.; Piao, Z. Experimental prediction model for the running-in state of a friction system based on chaotic characteristics and BP neural network. *Tribol. Int.* **2023**, *188*, 108846. [CrossRef]
22. Majumdar, A.; Bhushan, B. Role of fractal geometry in roughness characterization and contact mechanics of surfaces. *J. Tribol.* **1990**, *112*, 205–216. [CrossRef]
23. Sun, G.; Zhu, H.; Ding, C.; Jiang, Y.; Wei, C. On the boundedness of running-in attractors based on recurrence plot and recurrence qualification analysis. *Friction* **2019**, *7*, 432–443. [CrossRef]
24. Kennel, M.B.; Abarbanel, H.D. False neighbors and false strands: A reliable minimum embedding dimension algorithm. *Phys. Rev. E* **2002**, *66*, 026209. [CrossRef]
25. Goudarzi, S.; Anisi, M.H.; Kama, N.; Doctor, F.; Soleymani, S.A.; Sangaiah, A.K. Predictive modelling of building energy consumption based on a hybrid nature-inspired optimization algorithm. *Energy Build.* **2019**, *196*, 83–93. [CrossRef]
26. Tsonis, A.; Elsner, J.B. The weather attractor over very short timescales. *Nature* **1988**, *333*, 545–547. [CrossRef]
27. Lever, J.; Krzywinski, M.; Altman, N. Principal component analysis. *Nat. Methods* **2017**, *14*, 641–642. [CrossRef]
28. Grassberger, P.; Procaccia, I. Characterization of strange attractor. *Phys. Rev. Lett.* **1983**, *50*, 346. [CrossRef]
29. Lang, S.; Zhu, H.; Wei, C.; Zhou, W.; Li, Y. Study on characterization method of phase-point saturation based on the capacity dimension. *Fractals* **2022**, *30*, 2250035. [CrossRef]
30. Zhou, Y.; Wang, Z.; Zuo, X.; Zhao, H. Identification of wear mechanisms of main bearings of marine diesel engine using recurrence plot based on CNN model. *Wear* **2023**, *520*, 204656. [CrossRef]

Disclaimer/Publisher's Note: The statements, opinions and data contained in all publications are solely those of the individual author(s) and contributor(s) and not of MDPI and/or the editor(s). MDPI and/or the editor(s) disclaim responsibility for any injury to people or property resulting from any ideas, methods, instructions or products referred to in the content.